

# Lamellar eutectic growth with anisotropic interphase boundaries: Experimental study using the rotating directional solidification method

S. Akamatsu<sup>\*</sup>, S. Bottin-Rousseau, M. Şerefoglu<sup>1</sup>, G. Faivre

*Institut des Nanosciences de Paris, UPMC, CNRS, 4 Place Jussieu, 75252 Paris Cedex 05, France*

Available online 14 March 2012

## Abstract

We report on an experimental study of the effects of interphase boundary anisotropy on eutectic microstructures using a new methodology called rotating directional solidification (RDS), which consists of rotating a thin sample with respect to a fixed unidirectional thermal gradient. The systems used are thin, large eutectic grains of the  $\text{CBr}_4\text{-C}_2\text{Cl}_6$  and  $\text{In-In}_2\text{Bi}$  lamellar eutectic alloys. The shape of the observed RDS lamellar trajectories turns out to be a reproducible eutectic-grain-dependent feature, in agreement with the theoretical prediction that these trajectories are approximately homothetic to the Wulff form of the interphase boundary in the sample plane. We show that different modes of lamellar growth, ranging from quasi-isotropic to (crystallographically) locked, exist in different eutectic grains of the two alloys studied. A detailed characterisation of these modes is given, with particular attention to the as-yet poorly understood aspects of locked lamellar growth.

© 2012 Acta Materialia Inc. Published by Elsevier Ltd. All rights reserved.

**Keywords:** Eutectic solidification; Directional solidification; Solidification microstructures; Interphase boundaries

## 1. Introduction

The dramatic effects of a strong capillary anisotropy of interphase boundaries on eutectic directional-solidification patterns have long been noted [1,2], but have never been systematically studied. The property of the alloy that controls these effects is the Wulff plot of the interphase boundary in the reference frame of the laboratory. This Wulff plot varies from eutectic grain to eutectic grain, where the term “eutectic grain” (EG) designates both a given interphase orientation relationship – i.e. a heterophase bicrystal – and a given orientation of this bicrystal with respect to the directional-solidification setup. Careful experimentation requires a good crystallographic homogeneity of the samples, i.e. large-sized eutectic grains, and a small number of free orientational parameters. The use of thin-sample directional solidification, in addition to reducing the

dimensionality of the solidification pattern, allows one to grow nearly perfect large-sized eutectic grains [3]. Moreover, the use of a rotating directional solidification (RDS) stage, whereby a thin sample is rotated with respect to a fixed unidirectional thermal gradient, permits a single orientational parameter to be varied in situ while keeping the other parameters constant.

In this article, we present experimental observations performed by RDS in the  $\text{CBr}_4\text{-C}_2\text{Cl}_6$  and  $\text{In-In}_2\text{Bi}$  lamellar eutectic alloys. More specifically, we study the RDS lamellar patterns (i.e. the forms of the RDS lamellar trajectories) in a series of different eutectic grains in both alloys. Each RDS pattern turned out to be a reproducible feature of the EG to which it belonged, indicating that RDS patterns depend on only the characteristics of the Wulff plot of the interphase boundary. All the observed RDS patterns could be grouped into three categories with contrasting characteristics (quasi-isotropic, nearly locked, locked) independently of the alloy. We show that all the observations can be simply explained by means of the so-called “symmetric-pattern approximation”. This approximation is

<sup>\*</sup> Corresponding author.

*E-mail address:* [akamatsu@insp.jussieu.fr](mailto:akamatsu@insp.jussieu.fr) (S. Akamatsu).

<sup>1</sup> Present address: Department of Mechanical Engineering, Koç University, Rumeli Feneri Yolu, 34450 Sariyer, Istanbul, Turkey.

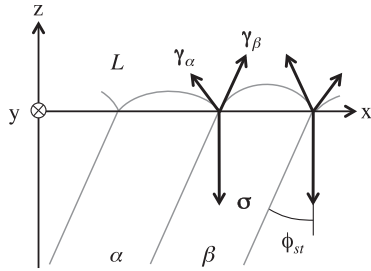


Fig. 1. Repeat unit of a lamellar eutectic pattern in a system with a strong interfacial anisotropy of the interphase boundary according to the symmetric-pattern approximation.  $\alpha$ ,  $\beta$ : eutectic phases.  $L$ : liquid.  $z$ : direction of the thermal gradient (growth direction).  $y$ : normal to the sample plane.  $x$ : average direction of the solid–liquid interface.  $\phi$ : inclination angle.  $\sigma$ : surface tension force of the interphase boundary.  $\gamma_\alpha$  and  $\gamma_\beta$ : surface tension forces of the supposedly isotropic solid–liquid interfaces.

discussed in detail in Ref. [4]. It can be summed up as follows. Based on general principles, an interphase boundary anisotropy is expected to break the spatiotemporal symmetry (symmetry with respect to the growth axis  $z$  and time invariance) distinctive of isotropic lamellar patterns. In other words, lamellar patterns should have asymmetric forms of their solid–liquid interfaces and travel laterally along the growth front (the lamellae left behind in the solid are inclined with respect to  $z$ ) in the presence of a strong interphase boundary anisotropy. However, on closer examination, it can be seen that the steady-state travelling velocity  $v_{st}$  of the patterns must be such that the solid–liquid interfaces remain nearly symmetric. The symmetric-pattern approximation consists of assuming that  $v_{st}$  is such that the solid–liquid interfaces are exactly symmetric or, equivalently, that the surface tension force  $\sigma$  of the interphase boundaries is parallel to  $z$  (Fig. 1; see Ref. [5] for a definition of  $\sigma$ ). As regards RDS experiments, it can be demonstrated that the symmetric-pattern approximation implies that the trajectories of the lamellae in the sample reference frame are homothetic to the two-dimensional (2-D) Wulff form of the interphase boundary in the EG under consideration. Thus, for instance, RDS lamellar trajectories should be almost circular in EGs where the interphase boundary anisotropy is negligible and faceted in EGs where the Wulff plot of the interphase boundary has cusp singularities (epitaxial EGs). This is the only consistent explanation for the familiar phenomenon of crystallographic locking of lamellar patterns. The report also includes a detailed description of the as-yet-unknown dynamical features of (crystallographically) locked lamellar patterns.

## 2. Experimental methods

### 2.1. Alloys and crucibles

The  $\text{CBr}_4\text{--C}_2\text{Cl}_6$  alloy has a eutectic plateau at  $T_E = 84.4^\circ\text{C}$ . The concentration of the eutectic liquid is  $C_E = 11.6\text{ mol.}\% \text{ C}_2\text{Cl}_6$ . The eutectic phases are a face-centred cubic phase ( $\alpha$ ) and a body-centred cubic phase ( $\beta$ ), with

concentrations of 8.8 and 18.5 mol.%  $\text{C}_2\text{Cl}_6$ , respectively [1,6]. The  $\text{In--In}_2\text{Bi}$  alloy has a eutectic plateau ( $T_E = 72.7^\circ\text{C}$ ,  $C_E = 22.2\text{ at.}\% \text{ Bi}$ ) between a face-centred tetragonal phase ( $\epsilon$ ) of concentration 11.5 at.% Bi and the hexagonal  $\text{In}_2\text{Bi}$  intermetallic compound [7]. The value of the Jackson–Hunt (JH) constant  $K_{JH} = \lambda_{JH} V^{0.5}$  at eutectic concentration, where  $\lambda_{JH}$  is the minimum undercooling spacing [1], was estimated to be  $13.8 \pm 0.5 \mu\text{m}^{1.5} \text{ s}^{-0.5}$  in  $\text{CBr}_4\text{--C}_2\text{Cl}_6$  [8] and  $7.07 \pm 0.35 \mu\text{m}^{1.5} \text{ s}^{-0.5}$  in  $\text{In--In}_2\text{Bi}$  [9]. Both  $\text{CBr}_4\text{--C}_2\text{Cl}_6$  and  $\text{In--In}_2\text{Bi}$  undergo a eutectoid transformation between  $T_E$  and room temperature, rendering post-mortem orientation measurements by X-ray diffraction problematic. We used nominally eutectic (in fact, slightly hypereutectic) alloys. The  $\text{In--In}_2\text{Bi}$  alloy was prepared from 99.999% pure indium and bismuth (Goodfellow), and the  $\text{CBr}_4\text{--C}_2\text{Cl}_6$  alloy from sublimated compounds. Thin crucibles were made of two 0.3 mm thick glass plates separated by 12  $\mu\text{m}$  thick plastic strips or 13  $\mu\text{m}$  diameter tungsten wires. It has been checked that convection flows in the liquid were suppressed in samples of this thickness. The in-plane dimensions of the rectangular space available for solidification were of  $15 \times 30 \text{ mm}^2$ . The crucibles were filled with molten alloys by capillarity ( $\text{CBr}_4\text{--C}_2\text{Cl}_6$ ) or by a vacuum suction method ( $\text{In--In}_2\text{Bi}$ ), then sealed at room temperature. Residual impurities contained in our samples induced the formation of eutectic cells at pulling velocities higher than  $5 \mu\text{m s}^{-1}$  in both alloys. The solidification rates considered herein are well below this threshold value.

### 2.2. Method of observation

The growth front was observed in real-time in the  $y$  direction with an inverted optical microscope. The transparent  $\text{CBr}_4\text{--C}_2\text{Cl}_6$  eutectic was observed in transmitted light. With this method, the contrast originates from the differences in refractive index of the different thermodynamic phases and reveals the interfaces. The  $\text{In--In}_2\text{Bi}$  eutectic was observed in reflected light through the lower glass wall of the crucible [10]. The differences in reflectivity between the different types of surfaces of contact gave rise to a contrast, which, after numerical enhancement, made the  $\epsilon$ -glass surfaces appear white, the  $\text{In}_2\text{Bi}$ -glass surfaces black and the liquid-glass surfaces grey. Perturbations (contrast effects making the  $\epsilon$ -glass contacts appear grey instead of white, barbules formed at the rear of the growth front) due to complex wetting and segregation phenomena at the sample walls [9] can be seen in some places in the micrographs, but are of no importance for our present purpose. Images were recorded with a monochrome digital camera and transferred to a PC for further analysis. A several millimetres wide region of interest was regularly scanned using the motorised stage of the microscope.

### 2.3. The rotating directional solidification stage

An RDS stage was built based on a model introduced by Oswald et al. [11] (Fig. 2). It comprises: (i) a thermal-gradient

Download English Version:

<https://daneshyari.com/en/article/7883334>

Download Persian Version:

<https://daneshyari.com/article/7883334>

[Daneshyari.com](https://daneshyari.com)